

Towards Open Intent Detection

Hanlei Zhang, Hua Xu, Shaojie Zhao, Qianrui Zhou

Abstract—The open intent detection problem is presented in this paper, which aims to identify known intents and detect open intent in natural language understanding. Current methods have two core challenges. On the one hand, the existing methods have limitations in learning robust representations to detect the open intent without any prior knowledge. On the other hand, there lacks an effective approach to learning the specific and compact decision boundary to distinguish the known intents and the open intent. This paper introduces an original pipeline framework, DA-ADB, to address these issues, which successively learns discriminative intent features with distance-aware strategy and appropriate decision boundaries adaptive to the feature space for open intent detection. The proposed method first leverages distance information to enhance the distinguishing capability of the intent representations. Then, it obtains discriminative decision boundaries adaptive to the known intent feature space by balancing both the empirical and open space risks. Extensive experiments show the effectiveness of distance-aware and boundary learning strategies. Compared with the state-of-the-art methods, our method achieves substantial improvements on three benchmark intent datasets. It also yields robust performance with different proportions of labeled data and known categories.

Index Terms—Intent detection, open classification, natural language understanding, representation learning, deep neural network.



1 INTRODUCTION

INTENT detection plays a critical role in natural language understanding (NLU), aiming to mine user purposes behind the text utterances. The traditional intent detection task is restricted to the closed-world classification. It assumes all the intent categories are accessible and has achieved great progress with a booming of effective methods for supervised classification [1], [2].

Nonetheless, due to the variety and uncertainty of the user needs, it is usually inapplicable to cover all intent categories. Taking Figure 1 as an example, there are two task-specific intents of booking flight and restaurant reservation. Ideally, we hope to identify each utterance within the two known intent categories, but some utterances may exist with unknown intents, such as asking time or place. We regard all the unknown intents as open intent. It is necessary to distinguish the utterances from known intents and the open intent as much as possible. For one thing, effectively detecting open intent can improve customer satisfaction by reducing false-positive errors while identifying known intents. For another thing, the detected open intent may be helpful to explore more of the user’s potential needs.

Traditional methods used support vector machine (SVM) to solve similar open set (world) problems in computer vision [3], [4], [5]. Scheirer et al. formally defined the open space risk as to the measure [3]. Fei and Liu [6] extended this problem to the text classification and reduced the open space risk by learning the closed spherical boundary of each positive class in the similarity space. However, the SVM-based methods failed to capture high-level semantics

User utterances	Intent Label
Book a flight from LA to Madrid.	Booking flight
Can you get me a table at Steve’s?	Restaurant reservation
Book Delta ticket Madison to Atlanta.	Booking flight
Schedule me a table at Red Lobster.	Restaurant reservation
.....
What time is it now?	Asking time (Open)
Where is the nearest school?	Asking place (Open)

Fig. 1. An example of open intent detection. Booking flight and Restaurant reservation are two known intents. We should identify them correctly while detecting the utterances with the open intent.

in modeling representations [7], [8]. With the booming of deep learning, researchers adopted deep neural networks (DNNs) to obtain more powerful feature representations. For example, Bendale and Boulton [7] designed an OpenMax layer after the penultimate layer of DNNs to estimate the open class probability. Hendrycks and Gimpel [9] detected the out-of-distribution samples with a threshold on the predicted probabilities of neural networks. Out-of-domain detection [10], [11] also detects the unknown samples, but its setting is different from ours, which fails to balance the performance of both known and open classes. Furthermore, most of the methods mentioned above need samples from the open class for training or evaluation [7], [9], [10], [11], [12]. Nevertheless, the high-quality labeled negative samples are hard to collect in intent detection scenarios. Therefore, researchers focused on a more challenging setting, which requires no need for open-class samples during training or evaluation [13], [14], [15], [16].

Concretely, we present the **open intent detection** problem, which is regarded as an $(K+1)$ -class classification task. The goal is to use only K -class known intents as prior

- H. Zhang, H. Xu, S. Zhao and Q. Zhou are with State Key Laboratory of Intelligent Technology and Systems, Department of Computer Science and Technology, Tsinghua University, Beijing 100084, China. E-mail: zhang-hl20@mails.tsinghua.edu.cn; xuhua@tsinghua.edu.cn; murrayzhao@163.com; zhougr18@mails.tsinghua.edu.cn.
- S. Zhao is with School of Information Science and Engineering, Hebei University of Science and Technology, Shijiazhuang 050018, China. Email: murrayzhao@163.com.
- Hua Xu is the corresponding author.

knowledge to detect the $(K+1)^{\text{th}}$ class open intent while ensuring the known intent identification performance.

The research on open intent detection is just beginning in recent years. A simple baseline [14] used a fixed confidence threshold on the maximum softmax probabilities of deep networks to detect the open intent. Shu et al. [13] modified the final layer with sigmoids and fitted Gaussian distribution to obtain more tight confidence thresholds of each known class. However, the probability-based methods are limited to distinguishing between known classes and the open class, especially with dense confidence scores. Researchers also tried to tackle this problem with feature-based methods. These methods designed specific model architectures for representation learning. For example, Lin and Xu [14] adopted the large margin cosine loss [17] to ensure intra-class compactness and inter-class separation and used local outlier factor (LOF) [18] to detect the low-density examples as the open class. Nevertheless, the embeddings optimized in cosine space may be less suitable for LOF [15]. Yan et al. [15] leveraged the Gaussian mixture model incorporating the class label information to obtain more suitable representations for anomaly detection, but the performance drops dramatically when the intent categories are with complicated semantics. Recently, Zhan et al. [16] constructed pseudo open class samples for $(K+1)$ -way training, yet the assumptions did not consider the fine-grained open-class data distribution.

There are two main difficulties in current open intent detection methods. Firstly, the representations trained on known intents may be not robust enough for detecting the unseen open class. Secondly, the decision conditions of these methods are still implicit and incompact to differentiate between both known and open intents.

To solve these problems, we propose a novel pipeline framework for open intent detection, which learns both discriminative representations and decision boundaries without any prior knowledge of the open intent. It first extracts deep intent representations from the pre-trained language model BERT [19] at the sentence level and calculates the centroids by averaging the samples of each known class. Then, it aims to perceive the distance information to learn representations with distinguishing capability. Specifically, each sample compares the Euclidean distances between its nearest and next closest centroids to compute the distance-aware coefficient. The coefficient is incorporated into the original intent representation to produce the meta-embedding. The magnitude of its meta-embedding reflects the hardness of each sample. That is, the larger magnitude corresponds to the easier sample with more confidence to differentiate the two nearest centroids. To achieve this, a cosine classifier [20] is adopted after the meta-embedding to consider the effect of the magnitude information, which is helpful to focus on harder samples with smaller magnitudes during training. In this way, the intent representations are calibrated to distance-aware concepts for more robust performance.

After representation learning, we aim to obtain specific and compact decision boundaries in the intent feature space. We suppose each known intent cluster is constrained in a spherical decision boundary to its centroid, which is helpful to reduce the open space risk [6]. The decision boundaries are determined by the radius of each ball area and should

be flexibly adaptive to different feature distributions. In particular, the boundary parameters are first initialized with standard normal distribution and then projected with a learnable activation function to get the radius of each decision boundary. The key factor is how to control the radius to learn compact decision boundaries for open intent detection, which should satisfy two conditions.

On the one hand, they should be broad enough to surround known intent samples as much as possible. On the other hand, they need to be tight enough to prevent the open intent samples from being identified as known intents. A new loss function is designed to address these issues, which optimizes the boundary parameters by balancing both the open space and empirical risk with known intent samples inside and outside the decision boundaries. With the boundary loss, the decision boundaries can automatically adapt to the intent feature space until balance. The boundary learning process is a post-processing method, which requires no modifying the original model architecture. It works even with the features trained on the simple softmax loss. The distance-aware strategy can further facilitate learning more discriminative representations for better performance.

Our contributions are summarized as follows:

- We clarify the formulation of the open intent detection problem and propose a novel and effective framework DA-ADB to tackle this problem.
- A distance-aware strategy is designed to capture the distinguishing ability of each sample, which is helpful to learn discriminative intent features.
- A novel post-processing method is proposed to learn tight decision boundaries adaptive to the feature space. To the best of our knowledge, it is the first attempt to automatically learn adaptive decision boundaries for detecting the unseen open class.
- Extensive experiments conducted on three challenging datasets show that our approach achieves consistently better and more robust results compared with the state-of-the-art methods.

The idea of adaptive decision boundary (ADB) was presented in a preliminary version of this paper published in the proceeding of the thirty-fifth AAAI conference (AAAI-21) [21]. In this paper, we extend the preliminary version in the following aspects:

- A novel method is introduced to incorporate the distance information into the intent representations. It is able to capture the hardness of each sample with the distance-aware coefficient for effective training.
- A series of experiments are conducted to show the advantages of injecting distance-aware concepts into intent representations for open intent detection.
- We formulate the open intent detection problem and enrich the introduction on related work. More baselines are reproduced and added to our experiments with detailed analysis.
- The experimental results are updated with our TEXTOIR platform [22], which has standard and unified interfaces for fair comparison ¹.

1. Full codes are available at <https://github.com/thuiar/TEXTTOIR>

2 RELATED WORK

2.1 Open World Classification

Open (world) classification is the pioneering work related to us. It aims to reject the negative samples while identifying positive samples. At first, researchers used SVM-based methods as the solutions. One-class SVM [23] was designed for binary open classification, which found the plane based on the positive training data and regarded the origin as the only member of the negative class. One-vs-all SVM [24] was designed for multi-class open classification, which trained the binary classifier for each class and treated the negative classified samples as the open class. Scheirer et al. [3] extended the method to computer vision and introduced the concept of open space risk. They introduced the 1-vs-Set Machine to improve generalization ability by compressing the decision space of 1-class SVM. Jain et al. [4] used a Weibull-calibrated multi-class SVM to estimate the posterior probability satisfying the statistical Extreme Value Theory (EVT). Scheirer et al. [5] presented a Compact Abating Probability (CAP) model, which further improved the performance of Weibull-calibrated SVM by truncating the abating probability. However, the methods above need negative samples to obtain decision boundaries.

As SVM-based methods have difficulties in capturing advanced pattern semantic concepts [8], researchers used deep neural networks for open classification. OpenMax [7] fit Weibull distribution to the outputs of the penultimate layer but still needed negative samples for selecting the best hyper-parameters. MSP [9] calculated the softmax probability of known samples and rejected the low confidence as the unknown samples with a threshold. ODIN [12] used temperature scaling and input pre-processing to enlarge the differences between known and unknown samples. Nevertheless, both of them [9], [12] need unknown samples to select the confidence threshold artificially. DOC [13] used the output layer of sigmoids and calculated the confidence thresholds based on Gaussian statistics, but it performs worse when the output probabilities are not discriminative.

2.2 Out-of-domain Detection

Out-of-domain detection is a similar task related to ours. Kim and Kim [10] jointly trained the in-domain classifier and out-of-domain detector, but the method needs samples of out-of-domain utterances. Yu et al. [25] adopted adversarial learning to generate positive and negative samples for training the classifier. Ryu et al. [26] used a generative adversarial network (GAN) to train on the in-domain samples and detected the out-of-domain samples with a discriminator. Zheng et al. [11] used a GAN-based generator to produce pseudo out-of-domain samples of discrete token sequences. Yet, it has been shown that deep generative models have limitations in learning high-level semantics on the discrete text data [27]. It is also important to note that the goal of out-of-domain detection is different from our task, which does not need to balance the performance of both known and open classes.

2.3 Intent Detection

Intent detection is a prevalent task in NLU. For example, the joint slot filling and intent detection task [28], [29], [30] has

been studied widely and achieved remarkable performance on typical benchmark datasets [31], [32]. Though more challenging intent benchmark datasets were proposed in recent years [33], [34], the powerful pre-trained language model still has excellent performance under the assumption of closed world classification [33].

However, collecting many labeled samples for each intent category is labor-intensive and time-consuming. A more realistic setting is some open (unknown) intent samples mixed with the known intents. Similar works have been explored to detect open intent. Brychcin and Král [35] proposed an unsupervised method to model intents but failed to utilize the prior knowledge of known intents. Xia et al. [36] performed intent detection with the zero-shot learning method, but the zero-shot setting contains only new intent classes during testing.

The open intent detection task has attracted attention in recent years. Lin and Xu [14] made the first trial on this problem. They learned deep intent features with the margin loss and detected the open intent with LOF. Yan et al. [15] replaced the margin loss with the Gaussian mixture loss for learning better embeddings, but the performance largely depends on the class-label semantics. Moreover, the density-based algorithm is unable to construct specific decision boundaries. Zhan et al. [16] regarded different (pseudo) open intents as one class during training, but it may lead to the collapse with intents of disparate semantics.

3 PROBLEM FORMULATION

In open intent detection we are given an intent label set I and a data set D . The intent label set $I = \{I^{\text{Known}}, \text{Open}\}$, where $I^{\text{Known}} = \{I_1, \dots, I_K\}$ is the known intent label set and K is the number of known intents. Notably, there may be multiple remaining intent labels in the initial label set $I \setminus \{I^{\text{Known}}\}$, as indicated in [37], [38]. In this problem, the non-known intents are all assigned the unified **Open** label.

The data set $D = \{D^{\text{Train}}, D^{\text{Valid}}, D^{\text{Test}}\}$ consists of training, validation and testing sets. Each subset (e.g., D^{Train}) contains a set of labeled samples (s_i, y_i) , where s_i is the i^{th} utterance, and y_i is its intent label.

The intent label set for both D^{Train} and D^{Valid} is I^{Known} , while for D^{Test} is I . The training and validation sets contain merely known intent samples, and the unseen open intent samples only exist in the testing set. The goal of open intent detection is to leverage the K -class known intents as prior knowledge to both identify known intents and detect the $(K+1)^{\text{th}}$ class open intent.

4 THE PROPOSED APPROACH

This section presents a novel framework to learn friendly intent representations and appropriate decision boundaries for open intent detection. It contains four main steps, intent representation, distance-aware representation learning, adaptive decision boundary learning, and open classification. Figure 2 shows the overall architecture of our proposed approach.

4.1 Intent Representation

The pre-trained BERT language model is adopted to extract deep intent features. Given the i^{th} input utterance \mathbf{s}_i , we get all its token embeddings $[CLS, Tok_1, \dots, Tok_M] \in \mathbb{R}^{(M+1) \times H}$ from the last hidden layer of BERT. As suggested in [37], we perform mean-pooling on these token embeddings to synthesize the semantic features in the utterance and get the averaged representation $\mathbf{x}_i \in \mathbb{R}^H$:

$$\mathbf{x}_i = \text{mean-pooling}([CLS, Tok_1, \dots, Tok_M]), \quad (1)$$

where CLS is a special classification token, M is the sequence length and H is the hidden layer size 768. To further strengthen feature extraction capability, we feed \mathbf{x}_i to a dense layer h to get the intent representation $\mathbf{z}_i \in \mathbb{R}^D$:

$$\mathbf{z}_i = h(\mathbf{x}_i) = \sigma(W_h \mathbf{x}_i + b_h), \quad (2)$$

where D is the feature dimension, σ is the ReLU activation function, $W_h \in \mathbb{R}^{H \times D}$ and $b_h \in \mathbb{R}^D$ respectively denote the weights and the bias term of layer h .

4.2 Distance-aware Representation Learning

A new distance-aware representation learning strategy is introduced to learn discriminative intent features. In this method, the centroids of each known class are first calculated and then used to compute the distance-aware coefficient of each sample to obtain the meta-embedding. After the meta-embedding, a cosine classifier is utilized to enable each sample to perceive the distance information.

4.2.1 Centroids Calculation

Let $S = \{(\mathbf{z}_i, y_i), \dots, (\mathbf{z}_N, y_N)\}$ be N known intent labeled examples. S_k denotes the set of feature vectors labeled with class k . The centroid $\mathbf{c}_k \in \mathbb{R}^D$ is the mean vector of embedded examples in S_k :

$$\mathbf{c}_k = \frac{1}{|S_k|} \sum_{(\mathbf{z}_i, y_i) \in S_k} \mathbf{z}_i, \quad (3)$$

where $|S_k|$ denotes the number of examples in S_k .

4.2.2 Meta Embedding with Distance-aware Concept

The initial intent representations have limitations in identifying whether an example is "easy" or "hard" during training, which is unfavorable for discriminative representation learning. To address this issue, we leverage the distance-aware concept to obtain the meta-embedding for enhancing the distinguishing ability.

For each example, the confidence of which known class it belongs to depends on the Euclidean distances between it and known-class centroids in the feature space. The index of the nearest centroid k_a is most likely to be its corresponding class, while the index of the second closest centroid k_b is the most confusing category to be classified. Thus, k_a and k_b are the two most informative centroid indexes to evaluate the distinguishing ability, and they are computed by:

$$k_a = \underset{k}{\operatorname{argmin}} \{ \|\mathbf{z}_i - \mathbf{c}_k\|_2 \}_{k \in I^{\text{Known}}}, \quad (4)$$

$$k_b = \underset{k}{\operatorname{argmin}} \{ \|\mathbf{z}_i - \mathbf{c}_k\|_2 \}_{k \in I^{\text{Known}} \setminus \{k_a\}}, \quad (5)$$

where $\|\mathbf{z}_i - \mathbf{c}_k\|_2$ denotes the Euclidean distance between \mathbf{z}_i and \mathbf{c}_k . An discriminative example should be close to its nearest centroid and far away from the next nearest centroid. Thus, the difference between $\|\mathbf{z}_i - \mathbf{c}_{k_b}\|_2$ and $\|\mathbf{z}_i - \mathbf{c}_{k_a}\|_2$ is used to reflect the separating capacity of \mathbf{z}_i . In particular, the distance-aware coefficient γ_i is defined as:

$$\gamma_i = \exp(\|\mathbf{z}_i - \mathbf{c}_{k_b}\|_2 - \|\mathbf{z}_i - \mathbf{c}_{k_a}\|_2) \text{ s.t. } \gamma_i \geq 1, \quad (6)$$

where $\exp(\cdot)$ enables an exponentially large reception field. It enhances the effect of differentiation and avoids the trivial solution when $\|\mathbf{z}_i - \mathbf{c}_{k_b}\|_2$ is close to $\|\mathbf{z}_i - \mathbf{c}_{k_a}\|_2$. Particularly, γ_i also suggests the difficulty of an example. An "easy" example is more confident to distinguish between the two nearest centroids and has a large γ_i . Yet, a "hard" example is more likely to be confused by the next nearest centroid and has a small γ_i .

To leverage the distance-aware concept, the intent representation \mathbf{z}_i is multiplied by γ_i to obtain the meta-embedding $\mathbf{z}_i^{\text{meta}}$:

$$\mathbf{z}_i^{\text{meta}} = \gamma_i \cdot \mathbf{z}_i. \quad (7)$$

4.2.3 Representation Learning

As the distance-aware coefficient is positively correlated with the magnitude of meta-embedding, it is natural to use the vector length to represent the distance-aware concept. For this purpose, the cosine classifier [20] is adopted to capture the distance information contained in the meta-embedding.

Specifically, the cosine similarity operator is used on the normalized meta-embeddings and weight vectors to compute the classification logits:

$$\phi(\mathbf{z}_i^{\text{meta}})^k = \alpha \cdot \cos(\mathbf{z}_i^{\text{meta}}, \mathbf{w}_k^*) = \alpha \cdot \frac{\mathbf{z}_i^{\text{meta}} \top \mathbf{w}_k^*}{\|\mathbf{z}_i^{\text{meta}}\| \|\mathbf{w}_k^*\|}, \quad (8)$$

where $\phi(\cdot)$ is the cosine classifier and $\phi(\cdot)^k$ are the output logits of the k^{th} class, α is a scalar hyper-parameter (detailed discussion can be seen in section 6.1.2). $\cos(\cdot)$ is the cosine similarity operator, which first normalizes the meta-embedding $\mathbf{z}_i^{\text{meta}}$ and the k^{th} class weight vector \mathbf{w}_k^* and then performs dot product operation.

In particular, $\mathbf{z}_i^{\text{meta}}$ and \mathbf{w}_k^* are applied by a non-linear squashing function [39] and L2 normalization to obtain $\overline{\mathbf{z}_i^{\text{meta}}}$ and $\overline{\mathbf{w}_k^*}$, respectively:

$$\overline{\mathbf{z}_i^{\text{meta}}} = \frac{\|\mathbf{z}_i^{\text{meta}}\|^2}{1 + \|\mathbf{z}_i^{\text{meta}}\|^2} \frac{\mathbf{z}_i^{\text{meta}}}{\|\mathbf{z}_i^{\text{meta}}\|}, \quad (9)$$

$$\overline{\mathbf{w}_k^*} = \frac{\mathbf{w}_k^*}{\|\mathbf{w}_k^*\|}, \quad (10)$$

where $\|\mathbf{z}_i^{\text{meta}}\|$ and $\|\mathbf{w}_k^*\|$ denote the magnitudes of $\mathbf{z}_i^{\text{meta}}$ and \mathbf{w}_k^* . The non-linear squashing function is helpful to reflect the magnitude information of a vector. It shrinks $\mathbf{z}_i^{\text{meta}}$ with a large magnitude to the length slightly below 1 and with a short magnitude to the length almost 0. The L2 normalization eliminates the affect of the weight vector magnitudes on classification logits.

The cosine classifier converts the magnitude information to discriminative classification outputs, and facilitates paying more attention on the "hard" example, which outputs lower classification scores with a smaller magnitude.

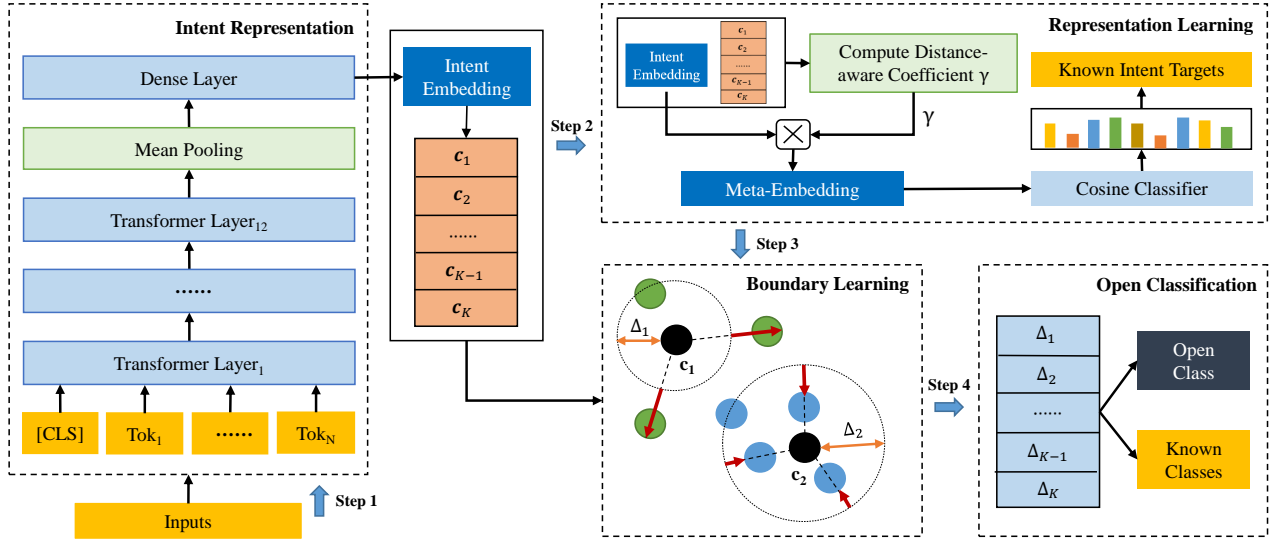


Fig. 2. The overall architecture of the proposed framework. Firstly, we use the pre-trained language model BERT to get intent embeddings and average them for each known class to obtain the centroids $\{c_i\}_{i=1}^K$. Then, the intent embeddings and centroids are leveraged to compute distance-aware coefficients, further multiplied over the original intent embeddings to yield the meta-embeddings. A cosine classifier learns the distance information with the known intent targets. Next, a new loss function is proposed to learn the radiuses of the decision boundaries $\{\Delta_i\}_{i=1}^K$ adaptive to the intent feature space. Finally, the centroids and decision boundaries are used for open intent detection.

Finally, we use the softmax loss \mathcal{L}_s to train the meta-embeddings under the supervision of known intent targets:

$$\mathcal{L}_s = -\frac{1}{N} \sum_{i=1}^N \log \frac{\exp(\phi(\mathbf{z}_i^{meta})y_i)}{\sum_{j=1}^K \exp(\phi(\mathbf{z}_i^{meta})j)}, \quad (11)$$

where y_i is the label of the i^{th} example. The initial intent representations can be calibrated to distance-aware concepts during training, and they are further used for learning decision boundaries.

4.3 Adaptive Decision Boundary Learning

An original approach to learning the adaptive decision boundary (ADB) is designed for open intent detection. We first formulate the decision boundary and then propose our boundary learning strategy for optimization.

4.3.1 Decision Boundary Formulation

It has been shown the superiority of the spherical shape boundary for open world classification [6], which greatly reduced the open space risk compared with the half-space binary linear classifier [23] and two parallel hyperplanes [3]. Inspired by this, we hope to construct ball-like decision boundaries in the deep feature space for open intent detection.

Due to the specificity of different intent categories, we aim to learn the corresponding decision boundaries for each known class. Concretely, for the k^{th} known class, the spherical decision boundary is determined by its corresponding centroid c_k and radius Δ_k , where $k \in \{1, 2, \dots, K\}$.

The centroid c_k is the average intent representation in class k , as defined in section 4.2.1. As the decision boundaries need to be adaptive to the intent feature space, the radius should be learnable to control the space range of the closed ball area. For this purpose, Δ_k is learned by the neural network with a boundary parameter $\widehat{\Delta}_k \in \mathbb{R}$. As

suggested in [40], the Softplus activation function is utilized as the mapping between Δ_k and $\widehat{\Delta}_k$:

$$\Delta_k = \log \left(1 + \exp(\widehat{\Delta}_k) \right). \quad (12)$$

The Softplus activation function is selected for the following reasons. Firstly, it guarantees differentiability with different $\widehat{\Delta}_k \in \mathbb{R}$ and supports stable optimization. Secondly, it ensures the radius Δ_k is above zero. Finally, it achieves linear characteristics like ReLU and allows for bigger Δ_k if necessary.

4.3.2 Boundary Learning

After formulating the centroid c_k and the radius Δ_k , a critical problem is how to find the suitable decision boundary with the prior knowledge of only known intent feature distributions. For each known class, a tight decision boundary should balance both empirical and open space risks [3]. That is, it is required a tradeoff between both inside and outside examples belonging to its class.

For each example (z_i, y_i) , if $\|z_i - c_{y_i}\|_2 > \Delta_{y_i}$, the decision boundaries are too small to contain their corresponding known intent examples, which may increase the empirical risk. In contrast, if $\|z_i - c_{y_i}\|_2 < \Delta_{y_i}$, though larger decision boundaries are beneficial to identify more known intent examples, they are more likely to introduce more open intent examples, which may increase the open space risk. Thus, the boundary loss \mathcal{L}_b is proposed to make a tradeoff:

$$\mathcal{L}_b = \frac{1}{N} \sum_{i=1}^N [\delta_i (\|z_i - c_{y_i}\|_2 - \Delta_{y_i}) + (1 - \delta_i) (\Delta_{y_i} - \|z_i - c_{y_i}\|_2)], \quad (13)$$

where δ_i is defined as:

$$\delta_i := \begin{cases} 1, & \text{if } \|z_i - c_{y_i}\|_2 > \Delta_{y_i}, \\ 0, & \text{if } \|z_i - c_{y_i}\|_2 \leq \Delta_{y_i}. \end{cases} \quad (14)$$

The boundary parameter $\widehat{\Delta}_k$ is updated regarding to \mathcal{L}_b as follows:

$$\widehat{\Delta}_k := \widehat{\Delta}_k - \eta \frac{\partial \mathcal{L}_b}{\partial \widehat{\Delta}_k}, \quad (15)$$

where η is the learning rate and $\frac{\partial \mathcal{L}_b}{\partial \widehat{\Delta}_k}$ is computed by:

$$\frac{\partial \mathcal{L}_b}{\partial \widehat{\Delta}_k} = \frac{\sum_{i=1}^N \delta'(y_i = k) \cdot (-1)^{\delta_i}}{\sum_{i=1}^N \delta'(y_i = k)} \cdot \frac{1}{1 + e^{-\widehat{\Delta}_k}}, \quad (16)$$

where $\delta'(y_i = k) = 1$ if $y_i = k$ and $\delta'(y_i = k) = 0$ if not. The denominator is guaranteed to be not zero by updating only $\widehat{\Delta}_k$ that has examples belonging to class k in a mini-batch.

The intrinsic properties of the boundary loss \mathcal{L}_b are in favor of learning adaptive decision boundaries. It calculates the Euclidean distance between each example and its centroid $\|z_i - c_k\|_2$ and uses the distance to compare with the radius of the corresponding decision boundary Δ_{y_i} , yielding the inside loss or outside loss. Specifically, the inside (or outside) loss is computed by the sum of the distances between the k^{th} class boundary-inside (or boundary-outside) examples and the boundary Δ_k . The suitable decision boundary is a balance between the inside and outside losses. When the inside loss is larger, the cumulative gradients are positive to make the decision boundary move inward. Similarly, when the outside loss is larger, the cumulative gradients are negative to make the decision boundary expand outward. This process enables the decision boundaries to be adaptive to the known intent feature space until balance.

4.4 Open Classification with Decision Boundary

After boundary learning, the learned decision boundaries and centroids are used for inference. For each example z_i , it is first recognized as the index k_a of the nearest centroid. Then, the corresponding decision boundary Δ_{k_a} is utilized to detect whether it belongs to the open intent:

$$k_a = \underset{k}{\operatorname{argmin}} \{d(z_i, c_k)\}_{k \in I^{\text{known}}}, \quad (17)$$

$$\hat{y} = \begin{cases} \text{Open, if } d(z_i, c_k) > \Delta_{k_a}; \\ k_a, \text{ if } d(z_i, c_k) \leq \Delta_{k_a}, \end{cases} \quad (18)$$

where I^{known} is the known intent label set as mentioned in section 3 and $d(z_i, c_k)$ denotes the Euclidean distance between z_i and c_k .

5 EXPERIMENTS

5.1 Datasets

We conduct experiments on three challenging real-world datasets to evaluate our approach. The detailed statistics are shown in Table 1.

BANKING A fine-grained dataset in the banking domain [33]. It contains 77 intents and 13,083 customer service queries.

OOS A dataset for intent classification and out-of-scope prediction [34]. It contains 150 intents, 22,500 in-domain queries and 1,200 out-of-domain queries.

StackOverflow A dataset published in Kaggle.com. It contains 3,370,528 technical question titles. We use the processed dataset [41], which has 20 different classes and 1,000 samples for each class.

5.2 Baselines

The state-of-the-art of open intent detection and open world classification methods are used as baselines, including MSP [9], SEG [15], LOF [18], DOC [13] OpenMax [7], DeepUnk [14], $(K+1)$ -way discriminative training [16]. We also compare with a variant of our method, ADB, which does not leverage distance information for representation learning.

The open set detection method OpenMax in computer vision is adapted to our task. It first uses the softmax loss to train a classifier on the known intents and then fits a Weibull distribution to the classifier's output logits. The confidence scores are finally calibrated with the OpenMax Layer.

In particular, MSP and OpenMax need samples from the open class for training or evaluation, which is inapplicable in our task. Therefore, we adopt the default hyper-parameters of OpenMax and use the same confidence threshold (0.5) as in [14] for MSP.

For a fair comparison between baselines and our approach, the detection methods are involved in evaluation rather than just testing. The backbones of all the methods are replaced with the same BERT model as ours.

5.3 Evaluation Metrics

For open intent detection, the accuracy score (ACC) and the macro F1-score over all classes (F1) are used to evaluate the overall performance. The macro F1-score over known classes ($F1_{\text{known}}$) and over the open class ($F1_{\text{open}}$) are used to evaluate the fine-grained performance.

Given a set of classes $C = \{C_1, \dots, C_K, C_{K+1}\}$, where K is the number of known classes and C_{K+1} is the open class. The macro F1-score over all classes (F1) is computed by:

$$F1 = 2 \times \frac{P \times R}{P + R}, \quad (19)$$

$$P = \frac{\sum_{i=1}^{K+1} P_{C_i}}{K+1}, \quad R = \frac{\sum_{i=1}^{K+1} R_{C_i}}{K+1}, \quad (20)$$

$$P_{C_i} = \frac{TP_{C_i}}{TP_{C_i} + FP_{C_i}}, \quad R_{C_i} = \frac{TP_{C_i}}{TP_{C_i} + FN_{C_i}} \quad (21)$$

where P and R are the macro precision score and the macro recall score over $K+1$ classes. P_{C_i} and R_{C_i} are the precision score and recall score on the C_i class. TP_{C_i} , FP_{C_i} and FN_{C_i} are the true positives, false positives and false negatives of the C_i class, respectively. Similarly, the macro f1-score over known classes ($F1_{\text{known}}$) and the open class ($F1_{\text{open}}$) are computed by:

$$F1_{\text{known}} = 2 \times \frac{P_{\text{known}} \times R_{\text{known}}}{P_{\text{known}} + R_{\text{known}}}, \quad (22)$$

$$P_{\text{known}} = \frac{\sum_{i=1}^K P_{C_i}}{K}, \quad R_{\text{known}} = \frac{\sum_{i=1}^K R_{C_i}}{K}, \quad (23)$$

$$F1_{\text{open}} = 2 \times \frac{P_{C_{K+1}} \times R_{C_{K+1}}}{P_{C_{K+1}} + R_{C_{K+1}}}, \quad (24)$$

where P_{C_i} and R_{C_i} are computed the same as in Eq. 21.

TABLE 1
Statistics of BANKING, OOS and StackOverflow datasets. # indicates the total number of utterances.

Dataset	Classes	#Training	#Validation	#Test	Vocabulary Size	Length (max / mean)
BANKING	77	9,003	1,000	3,080	5,028	79 / 11.91
OOS	150	15,000	3,000	5,700	8,376	28 / 8.31
StackOverflow	20	12,000	2,000	6,000	17,182	41 / 9.18

TABLE 2
Overall performance of open intent detection with different known class ratios (25%, 50% and 75%) and their mean scores on three datasets. The proposed method DA-ADB and its variant ADB are significantly better than others with p -value < 0.05 (†) and p -value < 0.1 (*) using t-test.

Datasets	Methods	25%		50%		75%		Mean	
		ACC	F1	ACC	F1	ACC	F1	ACC	F1
BANKING	MSP	41.84†	50.03†	59.80†	71.40†	75.90†	83.49†	59.18†	68.31†
	SEG	49.73†	52.03†	54.66†	62.86†	64.54†	69.37†	56.31†	61.42†
	OpenMax	47.76†	53.18†	65.53†	74.64†	78.32†	84.95†	63.87†	70.92†
	LOF	66.73†	63.38†	71.13†	76.26†	77.21†	83.64†	71.69†	74.43†
	DOC	70.31†	65.74†	74.60†	78.24†	78.94†	83.79†	74.62†	75.92†
	DeepUNK	70.68†	65.57†	71.01†	75.41†	74.73†	81.12†	72.14†	74.03†
	(K+1)-way	75.43†	68.31†	74.66†	78.13†	79.90†	85.22†	76.66†	77.22†
	ADB	79.94	72.08	79.52†	81.33†	81.35	86.08	80.27	79.83
	DA-ADB	81.09	73.65	81.64	82.60	81.18	85.68	81.30	80.64
OOS	MSP	49.78†	49.42†	62.71†	70.33†	72.86†	81.61†	61.78†	67.12†
	SEG	53.34†	47.57†	60.54†	62.51†	42.97†	42.49†	52.28†	50.86†
	OpenMax	70.27†	63.03†	80.22†	79.86†	75.36†	71.17†	75.28†	71.35†
	LOF	87.77	78.13	85.22†	83.86†	85.07†	87.20†	86.02†	83.06†
	DOC	86.08†	75.86†	85.19†	83.89†	85.93†	87.87†	85.73†	82.54†
	DeepUNK	87.18*	77.32*	84.95†	83.35†	84.61†	86.53†	85.58†	82.40†
	(K+1)-way	86.98†	76.58†	83.71†	82.85†	85.31†	87.90†	85.33†	82.44†
	ADB	88.21	78.14*	86.47†	85.11	86.98*	88.95	87.22†	84.07
	DA-ADB	89.49	79.95	87.96	85.64	87.46	88.47†	88.30	84.69
StackOverflow	MSP	27.91†	37.49†	53.23†	62.70†	73.20†	78.70†	51.45†	59.63†
	SEG	23.35†	34.59†	43.04†	55.10†	62.63†	69.86†	43.01†	53.18†
	OpenMax	38.97†	45.35†	60.27†	67.72†	75.78†	80.90†	58.34†	64.66†
	LOF	25.02†	35.29†	44.56†	56.57†	65.05†	71.87†	44.88†	54.58†
	DOC	57.75†	57.34†	73.88†	76.80†	80.55†	84.37†	70.73†	72.84†
	DeepUNK	40.03†	45.64†	55.46†	64.78†	71.56†	77.63†	55.68†	62.68†
	(K+1)-way	53.05†	53.12†	63.54†	69.26†	74.72†	79.47†	63.77†	67.28†
	ADB	86.70*	79.79†	86.51†	85.55†	82.84*	86.07†	85.35†	83.80†
	DA-ADB	89.03	82.81	87.79	86.92	83.63	86.89	86.82	85.54

5.4 Experimental Settings

Open intent detection follows the open-world setting [13], which keeps some classes as unknown (open) and integrates them back during testing. Specifically, the proportions of known classes to total categories are varied with 25%, 50%, and 75%. The remaining classes are regarded as one open class. All the datasets are divided into training, validation, and testing sets. The samples from the open class are removed from the training and evaluation sets and only exist in the testing set, as mentioned in section 3. To reduce the impact of different selected known intent categories on the performance, we report the average performance over ten runs of experiments for each known class ratio with random seeds of 0-9.

We employ the pre-trained language model BERT (bert-uncased, with 12-layer transformer) implemented in PyTorch [42] and adopt most of its suggested hyper-parameters for optimization. To improve the training effi-

ciency and achieve better performance, we freeze all but the last transformer layer parameters of BERT. The feature dimension D is 768, the training batch size is 128, and the learning rate is $2e-5$. For DA-ADB, the scalar α of the cosine classifier is 4, which is searched from $\{2, 4, 8, 16, 32, 64\}$ by combining both feature learning and open classification performance on the evaluation set. The boundary loss \mathcal{L}_b uses Adam [43] to optimize the boundary parameters at a learning rate of 0.05.

5.5 Results

The main experimental results of open intent detection are shown in Table 2 and Table 3, where the best results are highlighted in bold, and Student’s t-test is conducted to measure the significance of performance difference.

Table 2 shows the overall performance of the accuracy score (ACC) and macro F1-score (F1) over all classes. The proposed approach DA-ADB and its variant ADB

TABLE 3

Fine-grained performance of open intent detection with different known class ratios (25%, 50%, 75%) and their mean scores on three datasets. The proposed method DA-ADB and its variant ADB are significantly better than others with p -value < 0.05 (†) and p -value < 0.1 (*) using t-test.

Datasets	Methods	25%		50%		75%		Mean	
		Open	Known	Open	Known	Open	Known	Open	Known
BANKING	MSP	38.84†	50.62†	42.13†	72.17†	41.64†	84.21†	40.87†	69.00†
	SEG	52.97†	51.98†	42.35†	63.40†	37.58†	69.92†	44.30†	61.77†
	OpenMax	48.52†	53.42†	55.03†	75.16†	53.02†	85.50†	52.19†	71.36†
	LOF	72.64†	62.89†	66.81†	76.51†	54.19†	84.15†	64.55†	74.52†
	DOC	76.64†	65.16†	72.66†	78.38†	63.51†	84.14†	70.94†	75.89†
	DeepUNK	76.98†	64.97†	67.80†	75.61†	50.57†	81.65†	65.12†	74.08†
	(K+1)-way	81.52†	67.61†	72.38†	78.29†	62.13†	85.62	72.01†	77.17†
	ADB	85.57	71.37	79.32†	81.38†	67.32*	86.40	77.40†	79.72
	DA-ADB	86.49	72.97	82.10	82.61	69.51	85.69*	79.37	80.51
	OOS	MSP	54.74†	49.28†	57.49†	70.50†	56.26†	81.83†	56.16†
SEG		60.59†	47.23†	61.13†	62.52†	41.60†	42.50†	54.44†	50.75†
OpenMax		77.51†	62.65†	82.15†	79.83†	75.18†	71.14†	78.28†	71.21†
LOF		91.96	77.77	87.57†	83.81†	82.81†	87.24†	87.45†	82.94†
DOC		90.78†	75.46†	87.45†	83.84†	83.87†	87.91†	87.37†	82.40†
DeepUNK		91.61†	76.95†	87.48†	83.30†	82.67†	86.57†	87.25†	82.27†
(K+1)-way		91.44†	76.19†	85.84†	82.82†	82.39†	87.95*	86.56†	82.32†
ADB		92.30	77.77*	88.54†	85.06	84.81†	88.99	88.55†	83.94
DA-ADB		93.20	79.60	90.14	85.58	86.09	88.49†	89.81	84.56
StackOverflow		MSP	11.66†	42.66†	26.94†	66.28†	37.86†	81.42†	25.49†
	SEG	4.36†	40.63†	4.72†	60.14†	6.38†	74.09†	5.15†	58.29†
	OpenMax	34.52†	47.51†	46.11†	69.88†	49.69†	82.98†	43.44†	66.79†
	LOF	7.14†	40.92†	5.18†	61.71†	5.22†	76.31†	5.85†	59.65†
	DOC	62.50†	56.30†	71.18†	77.37†	65.32†	85.64†	66.33†	73.10†
	DeepUNK	36.87†	47.39†	35.80†	67.67†	34.38†	77.63†	35.68†	65.19†
	(K+1)-way	56.31†	52.48†	53.68†	70.81†	47.57†	81.60†	52.52†	68.30†
	ADB	90.91*	77.56†	87.72†	85.33†	74.02	86.87†	84.22†	83.25†
	DA-ADB	92.61	80.84	88.86	86.72	74.66	87.71	85.38	85.09

achieve the best results on all settings and outperform other baselines by a significant large margin. Compared with ADB, DA-ADB yields substantial improvements with fewer known intents (25% and 50%) and achieves competitive results with more known intents (75%), which indicates the effectiveness of the distance-aware concept for representation learning. Compared with the state-of-the-art methods, the average performance of three known-class ratios shows that DA-ADB improves ACC by 4.64% on BANKING, 2.28% on OOS, and 16.09% on StackOverflow, respectively.

Table 3 shows the fine-grained performance of the macro F1-score over known classes ($F1_{\text{known}}$) and the open class ($F1_{\text{open}}$). Our approach not only achieves significant improvements to detect the open intent but also largely enhances the known intent identification performance. We notice that ADB gains the best results over all baselines. It indicates the learned decision boundaries are suitable to balance both the empirical and open space risks. On this basis, DA-ADB learns more friendly intent representations with the aid of distance information, which is helpful to increase 1% ~ 2% scores for open intent detection.

Moreover, it is worth noting that the improvements on the StackOverflow dataset are much more drastic than the other two datasets. We suppose the reason is that the characteristics of StackOverflow put forward higher requirements for open intent detection. Existing methods are limited to distinguishing the difficult semantic intents

such as technical question titles in StackOverflow without learning discriminative intent representations and decision boundaries.

6 DISCUSSION

6.1 Effect of Distance-aware Representation Learning

In this section, we first visualize the intent representations to verify the effectiveness of the distance-aware representation learning strategy and then analyze the influence of the hyper-parameter α as mentioned in section 4.2.3.

6.1.1 Visualization of Intent Representations

In Figure 3, we use t-SNE [44] to visualize the learned intent representations on the testing set of the BANKING dataset. It is shown that the vanilla intent representations of known intents are dispersed, which may result in fuzzy boundaries between adjacent clusters. The open intent representations are distributed haphazardly throughout the feature space, which easily leads to confusion between open and known intent samples.

In contrast, the intent representations learned with distance-aware concepts are more discriminative. The known intent samples are with intra-class compactness and inter-class separation properties. Surprisingly, the distributions of open intent samples are more concentrated to be far away from many known intents, which is beneficial to be better detected.

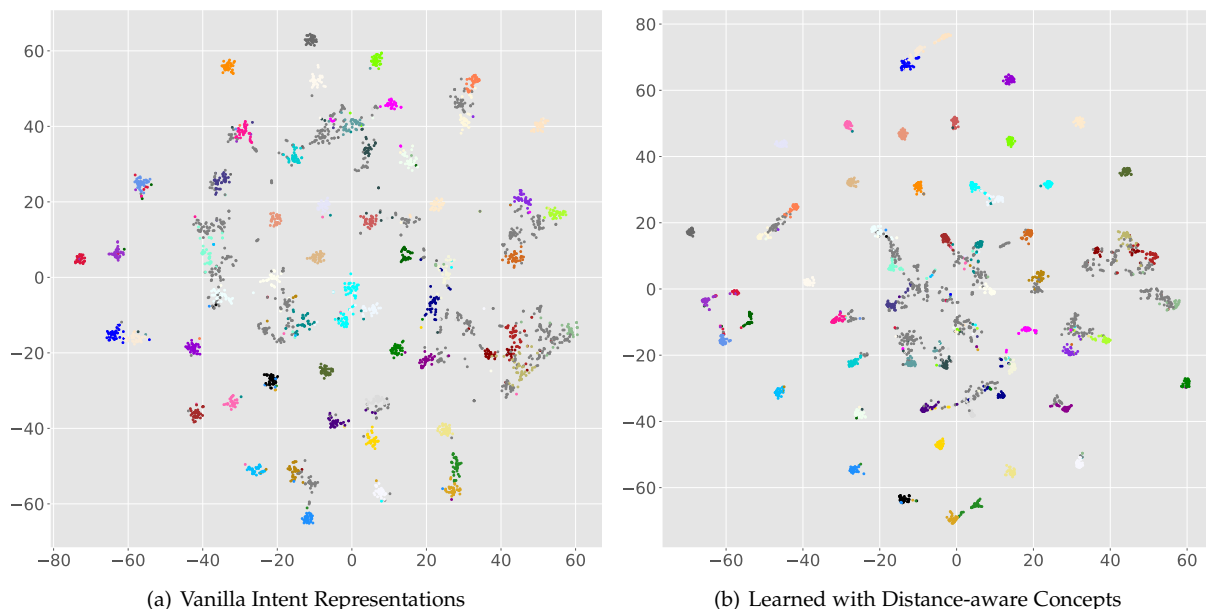


Fig. 3. Visualization of Learned Intent Representations on the BANKING dataset. The open intent is marked in gray, and known intents are marked in other colors.

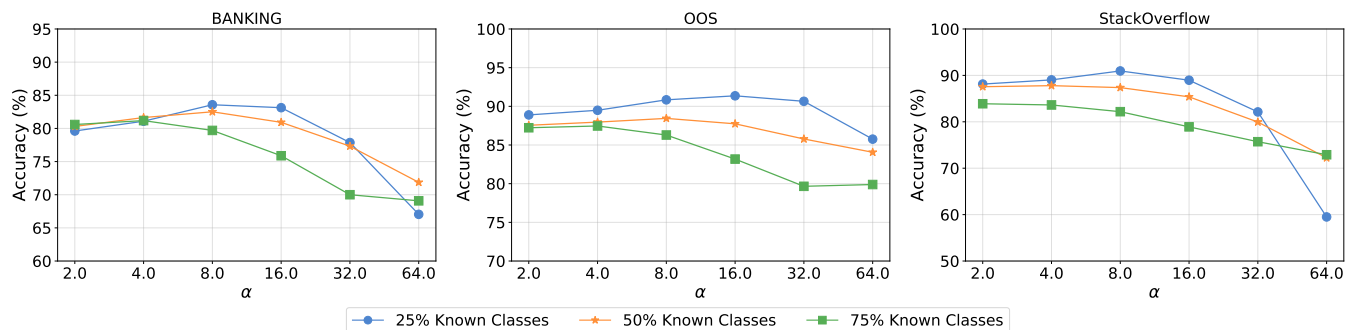


Fig. 4. Influence of α on three datasets with different known class ratios.

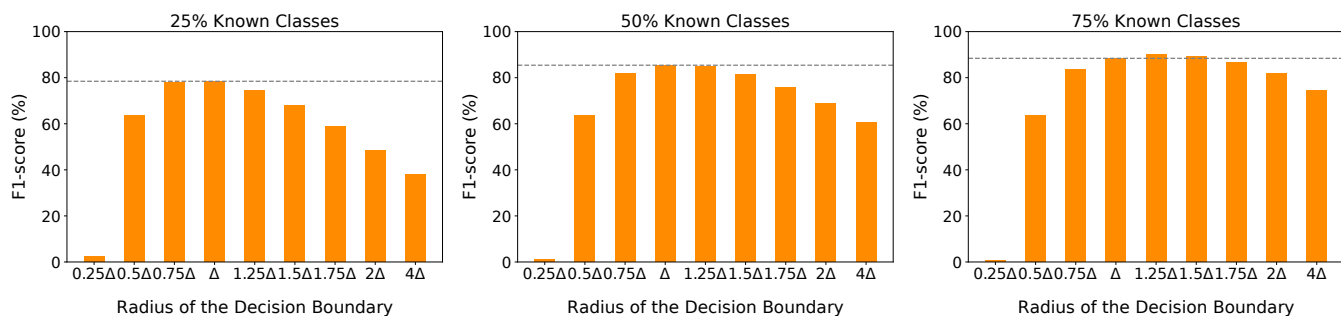


Fig. 5. Influence of the decision boundary on the OOS dataset with different known class ratios.

6.1.2 Analysis of Hyper-parameter α

In Figure 4, we use the accuracy score as the metric and show the effect of α on three datasets with different known class ratios. The hyper-parameter α is used to control the logits of the cosine classifier within a desirable range. Intuitively, a large α is better as it can scale the cosine similarity scores and further increase the peakiness of the softmax distribution [20] to enhance the discrimination of the intent representations.

However, it is interesting to observe that though a larger α may achieve higher performance with fewer known intents (25%), the performance drops rapidly with more known intents (75%). We suppose the reason is that the discriminative feature distributions are helpful to learn compact decision boundaries, which works better when there are fewer known intent samples. Nevertheless, it may not be good to identify more known intent samples with tight decision boundaries.

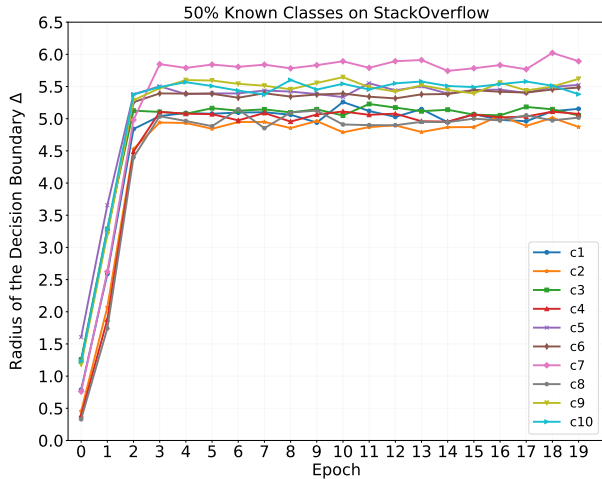


Fig. 6. The boundary learning process.

6.2 Effect of Adaptive Decision Boundary Learning

6.2.1 Analysis of Radius of Decision Boundary Δ

To verify the discrimination of the learned decision boundary, we use different ratios of Δ (radius of the decision boundary) for open intent detection on the BANKING dataset and show the results in Figure 5. The dotted lines indicate the performance with our learned Δ .

DA-ADB achieves the best or competitive performance with Δ among all assigned decision boundaries, which verifies the tightness of the learned decision boundary. Though 1.25Δ is slightly better on 75% known classes, it is lower on the other two settings. We notice that the performance of open intent detection is sensitive to the size of the decision boundaries. Overcompact decision boundaries will increase the open space risk by misclassifying more known intent samples to the open intent. Correspondingly, overrelaxed decision boundaries will increase the empirical risk by misclassifying more open intent samples as known intents. The two cases both perform worse compared with Δ .

6.2.2 Boundary Learning Process

Figure 6 shows the decision boundary learning process. At first, most parameters are assigned small values near zero after initialization, which leads to a small radius with the Softplus activation function. As the initial radius is too small, the empirical risk is dominant. Therefore, the radius of each decision boundary expands to contain more known intent samples belonging to its class. As the training process goes on, the radius of the decision boundary learns to be large enough to contain most of the known intents. However, the large radius will also introduce redundant open intent samples. In this case, the open space risk plays a dominant role, which prevents the radius from enlarging. Finally, the decision boundaries converge with a balance between empirical and open space risks.

6.3 Effect of Labeled Data

To investigate the influence of labeled data, we vary the labeled ratio in training set in the range of 0.2, 0.4, 0.6, 0.8, and 1.0. The accuracy score is used to evaluate the performance.

As shown in Figure 7, DA-ADB outperforms all the other baselines on three datasets on almost all settings. Besides, it keeps a more robust performance under different labeled ratios than other methods.

Notably, the probability-based methods (e.g., MSP, DOC, OpenMax, and $(K+1)$ -way) show better performance with less labeled data on many cases. We suppose the reason is that the predicted scores are in low-confidence with less prior knowledge for training, which is helpful to reject the open intent with the threshold. However, as the number of labeled data increases, these methods tend to be biased towards the known intents with the aid of strong feature extraction capability of DNNs [45] and suffer performance degradation. The performance of OpenMax is unstable as it computes centroids of each known class with only corrective positive training samples, and the qualities of centroids are easily influenced by the number. Compared with the aforementioned methods, $(K+1)$ -way achieves more robust performance by using pseudo samples as the open class.

In addition, the feature-based methods (e.g., SEG, LOF, DeepUnk) adopt a density-based novelty detection algorithm to perform open intent detection, which largely depends on the prior knowledge of labeled data, and their performance all drop dramatically with less labeled data. ADB also shows excellent and robust performance with suitable learned decision boundaries, but it performs worse on many settings without utilizing the distance information during feature learning.

7 CONCLUSIONS

In this paper, we formally present the open intent detection problem. This problem uses only known intents as prior knowledge, and the goal is not only to identify these known intents but also to detect the open intent. Obtaining friendly intent representations and appropriate decision boundaries are two critical challenges for open intent detection. To solve these problems, we propose a novel pipeline framework, DA-ADB, which learns discriminative features with distance-aware concepts and learns suitable decision boundaries by balancing both empirical and open space risks. We conducted extensive experiments on three benchmark datasets to show the superiority of the proposed method. Our approach yields significant improvements over state-of-the-art methods and achieves robust performance with different known intents and labeled data ratios.

ACKNOWLEDGMENTS

This paper is funded by National Natural Science Foundation of China (Grant No: 61673235). Sincerely, we thank the help and constructive feedback of Ting-En Lin, from DAMO Academy, Alibaba Group.

REFERENCES

- [1] L. Qin, T. Xie, W. Che, and T. Liu, "A survey on spoken language understanding: Recent advances and new frontiers," in *Proceedings of IJCAI*, 2021, pp. 4577–4584, survey Track.
- [2] H. Weld, X. Huang, S. Long, J. Poon, and S. C. Han, "A survey of joint intent detection and slot-filling models in natural language understanding," *arXiv preprint arXiv:2101.08091*, 2021.

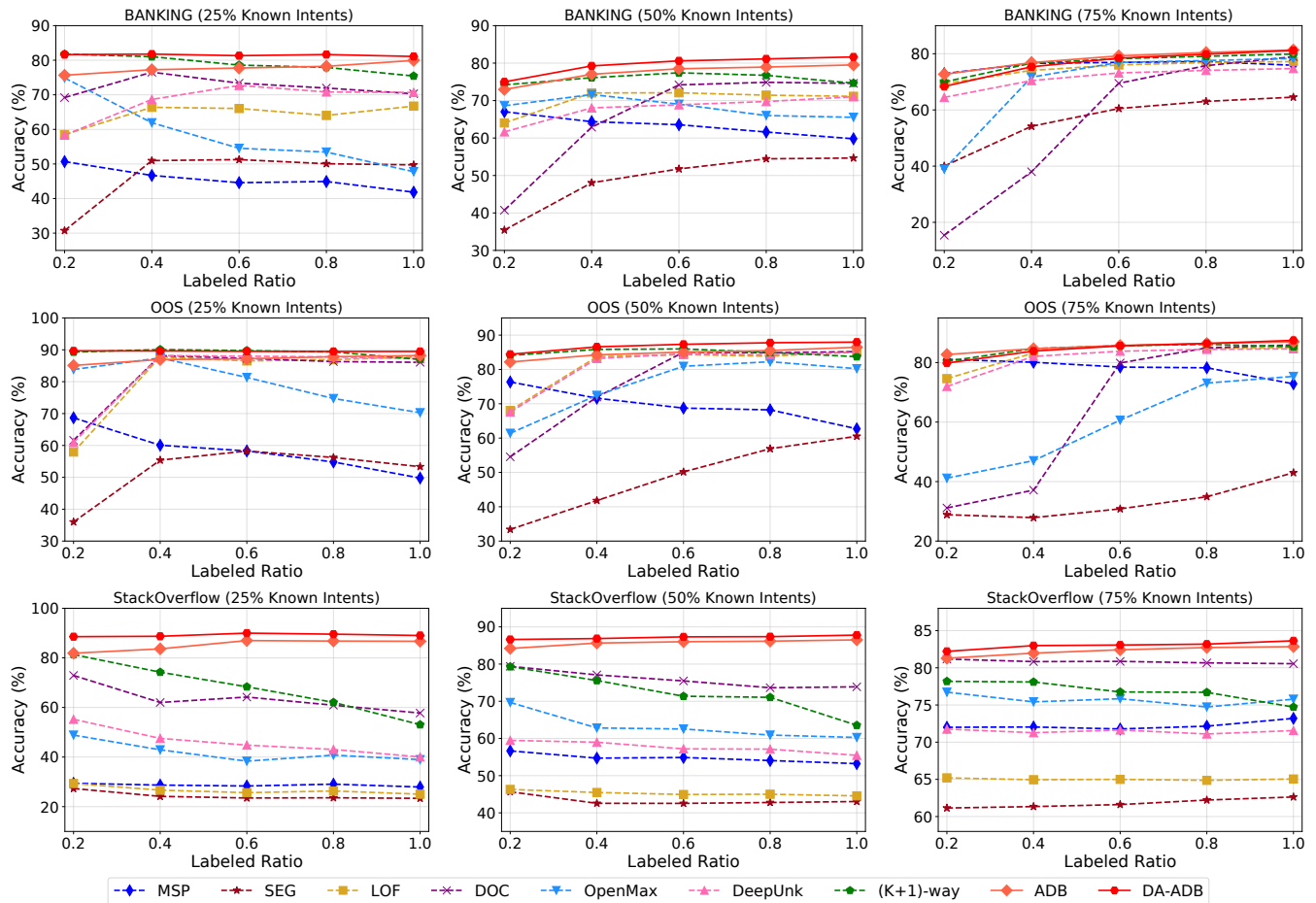


Fig. 7. Influence of the labeled ratio on the three datasets with different known class ratios.

- [3] W. J. Scheirer, A. de Rezende Rocha, A. Sapkota, and T. E. Boulton, "Toward open set recognition," *IEEE Transactions on Pattern Analysis and Machine Intelligence*, vol. 7, no. 35, pp. 1757–1772, 2013.
- [4] L. P. Jain, W. J. Scheirer, and T. E. Boulton, "Multi-class open set recognition using probability of inclusion," in *Proceedings of ECCV 2014*, D. Fleet, T. Pajdla, B. Schiele, and T. Tuytelaars, Eds. Springer International Publishing, 2014, pp. 393–409.
- [5] W. J. Scheirer, L. P. Jain, and T. E. Boulton, "Probability models for open set recognition," *IEEE Transactions on Pattern Analysis and Machine Intelligence*, vol. 36, no. 11, pp. 2317–2324, 2014.
- [6] G. Fei and B. Liu, "Breaking the closed world assumption in text classification," in *Proceedings of NAACL-HLT*, 2016, pp. 506–514.
- [7] A. Bendale and T. E. Boulton, "Towards open set deep networks," in *Proceedings of CVPR*, 2016, pp. 1563–1572.
- [8] T.-E. Lin and H. Xu, "A post-processing method for detecting unknown intent of dialogue system via pre-trained deep neural network classifier," *Knowledge-Based Systems*, vol. 186, p. 104979, 2019.
- [9] D. Hendrycks and K. Gimpel, "A baseline for detecting misclassified and out-of-distribution examples in neural networks," in *Proceedings of ICLR*, 2017.
- [10] J.-K. Kim and Y.-B. Kim, "Joint learning of domain classification and out-of-domain detection with dynamic class weighting for satisfying false acceptance rates," in *Proceedings of INTERSPEECH*, 2018, pp. 556–560.
- [11] Y. Zheng, G. Chen, and M. Huang, "Out-of-domain detection for natural language understanding in dialog systems," *IEEE/ACM Transactions on Audio, Speech, and Language Processing*, vol. 28, pp. 1198–1209, 2020.
- [12] S. Liang, Y. Li, and R. Srikant, "Enhancing the reliability of out-of-distribution image detection in neural networks," in *Proceedings of ICLR*, 2018.
- [13] L. Shu, H. Xu, and B. Liu, "Doc: Deep open classification of text documents," in *Proceedings of EMNLP*, 2017, pp. 2911–2916.
- [14] T.-E. Lin and H. Xu, "Deep unknown intent detection with margin loss," in *Proceedings of ACL*, 2019, pp. 5491–5496.
- [15] G. Yan, L. Fan, Q. Li, H. Liu, X. Zhang, X.-M. Wu, and A. Y. Lam, "Unknown intent detection using Gaussian mixture model with an application to zero-shot intent classification," in *Proceedings of ACL*, 2020, p. 1050–1060.
- [16] L.-M. Zhan, H. Liang, B. Liu, L. Fan, X.-M. Wu, and A. Y. Lam, "Out-of-scope intent detection with self-supervision and discriminative training," in *Proceedings of ACL*, 2021, pp. 3521–3532.
- [17] H. Wang, Y. Wang, Z. Zhou, X. Ji, D. Gong, J. Zhou, Z. Li, and W. Liu, "Cosface: Large margin cosine loss for deep face recognition," in *Proceedings of CVPR*, 2018, pp. 5265–5274.
- [18] M. M. Breunig, H.-P. Kriegel, R. T. Ng, and J. Sander, "Lof: identifying density-based local outliers," in *Proceedings of the ACM SIGMOD international conference on Management of data*, 2000, pp. 93–104.
- [19] J. Devlin, M.-W. Chang, K. Lee, and K. Toutanova, "Bert: Pre-training of deep bidirectional transformers for language understanding," in *Proceedings of NAACL-HLT*, 2019, pp. 4171–4186.
- [20] S. Gidaris and N. Komodakis, "Dynamic few-shot visual learning without forgetting," in *Proceedings of CVPR*, 2018, pp. 4367–4375.
- [21] H. Zhang, H. Xu, and T.-E. Lin, "Deep open intent classification with adaptive decision boundary," *Proceedings of AAAI*, vol. 35, no. 16, pp. 14374–14382, 2021.
- [22] H. Zhang, X. Li, H. Xu, P. Zhang, K. Zhao, and K. Gao, "TEXTOIR: An integrated and visualized platform for text open intent recognition," in *Proceedings of ACL*. Association for Computational Linguistics, 2021, pp. 167–174.
- [23] B. Schölkopf, J. C. Platt, J. Shawe-Taylor, A. J. Smola, and R. C. Williamson, "Estimating the support of a high-dimensional distribution," *Neural computation*, vol. 13, no. 7, pp. 1443–1471, 2001.
- [24] R. M. Rifkin and A. Klautau, "In defense of one-vs-all classification," *Journal of Machine Learning Research*, vol. 5, pp. 101–141, 2004.

- [25] Y. Yu, W.-Y. Qu, N. Li, and Z. Guo, "Open-category classification by adversarial sample generation," in *Proceedings of IJCAI*, 2017, pp. 3357–3363.
- [26] S. Ryu, S. Koo, H. Yu, and G. G. Lee, "Out-of-domain detection based on generative adversarial network," in *Proceedings of EMNLP*, 2018, pp. 714–718.
- [27] E. Nalisnick, A. Matsukawa, Y. W. Teh, D. Gorur, and B. Lakshminarayanan, "Do deep generative models know what they don't know?" in *Proceedings of ICLR*, 2019.
- [28] C. Zhang, Y. Li, N. Du, W. Fan, and P. Yu, "Joint slot filling and intent detection via capsule neural networks," in *Proceedings of ACL*, 2019, p. 5259–5267.
- [29] H. E. P. Niu, Z. Chen, and M. Song, "A novel bi-directional interrelated model for joint intent detection and slot filling," in *Proceedings of ACL*, 2019, pp. 5467–5471.
- [30] L. Qin, W. Che, Y. Li, H. Wen, and T. Liu, "A stack-propagation framework with token-level intent detection for spoken language understanding," in *Proceedings of EMNLP*, 2019, p. 2078–2087.
- [31] C. T. Hemphill, J. J. Godfrey, and G. R. Doddington, "The ATIS spoken language systems pilot corpus," in *Proceedings of a Workshop on Speech and Natural Language*, 1990, pp. 96–101.
- [32] A. Coucke, A. Saade, A. Ball, T. Bluche, A. Caulier, D. Leroy, C. Doumouro, T. Gisselbrecht, F. Caltagirone, T. Lavril *et al.*, "Snips voice platform: an embedded spoken language understanding system for private-by-design voice interfaces," *arXiv preprint arXiv:1805.10190*, 2018.
- [33] I. Casanueva, T. Temcinas, D. Gerz, M. Henderson, and I. Vulic, "Efficient intent detection with dual sentence encoders," in *Proceedings of ACL WorkShop*, 2020.
- [34] S. Larson, A. Mahendran, J. J. Peper, C. Clarke, A. Lee, P. Hill, J. K. Kummerfeld, K. Leach, M. A. Laurenzano, L. Tang, and J. Mars, "An evaluation dataset for intent classification and out-of-scope prediction," in *Proceedings of EMNLP-IJCNLP*, 2019, pp. 1311–1316.
- [35] T. Brychcin and P. Král, "Unsupervised dialogue act induction using gaussian mixtures," in *Proceedings of EACL*, 2017, pp. 485–490.
- [36] C. Xia, C. Zhang, X. Yan, Y. Chang, and P. Yu, "Zero-shot user intent detection via capsule neural networks," in *Proceedings of EMNLP*, 2018, pp. 3090–3099.
- [37] T.-E. Lin, H. Xu, and H. Zhang, "Discovering new intents via constrained deep adaptive clustering with cluster refinement," in *Proceedings of AAAI*, 2020, pp. 8360–8367.
- [38] H. Zhang, H. Xu, T.-E. Lin, and R. Lyu, "Discovering new intents with deep aligned clustering," *Proceedings of the AAAI*, pp. 14365–14373, 2021.
- [39] S. Sabour, N. Frosst, and G. E. Hinton, "Dynamic routing between capsules," in *Proceedings of NIPS*, vol. 30, 2017, pp. 3856–3866.
- [40] M. Tapaswi, M. T. Law, and S. Fidler, "Video face clustering with unknown number of clusters," in *Proceedings of ICCV*, 2019, pp. 5026–5035.
- [41] J. Xu, P. Wang, G. Tian, B. Xu, J. Zhao, F. Wang, and H. Hao, "Short text clustering via convolutional neural networks," in *Proceedings of NAACL-HLT*, 2015, pp. 62–69.
- [42] T. Wolf, L. Debut, V. Sanh, J. Chaumond, C. Delangue, A. Moi, P. Cistac, T. Rault, R. Louf, M. Funtowicz, and J. Brew, "Hugging-face's transformers: State-of-the-art natural language processing," *arXiv preprint arXiv:1910.03771*, 2019.
- [43] D. P. Kingma and J. Ba, "Adam: A method for stochastic optimization," *arXiv preprint arXiv:1412.6980*, 2014.
- [44] L. Van der Maaten and G. Hinton, "Visualizing data using t-sne." *Journal of machine learning research*, vol. 9, no. 11, 2008.
- [45] A. Nguyen, J. Yosinski, and J. Clune, "Deep neural networks are easily fooled: High confidence predictions for unrecognizable images," in *Proceedings of CVPR*, 2015, pp. 427–436.